A Symbol-by-Symbol Cooperative Diversity Scheme for Relay-Assisted UWB Communications with PPM

Chadi Abou-Rjeily, *Member IEEE*

***Abstract*—In this paper, we propose a novel cooperation strategy for coherent Impulse-Radio Ultra-Wideband (IR-UWB) communication systems with one relay. While non-orthogonal cooperation in narrow-band wireless networks often requires deploying distributed space-time codes with joint encoding of several symbols at the source and relays and joint decoding of these symbols at the destination, the proposed non-orthogonal cooperation scheme constitutes the first known symbol-by-symbol-based scheme where cooperation is entirely realized within one symbol duration. This follows from the fact that the proposed strategy is adapted to the structure of the Pulse Position Modulation (PPM) that constitutes the most popular modulation scheme associated with UWB transmissions. We also propose a simple and efficient power allocation strategy that further boosts the performance of the proposed cooperation strategy. The error performance of the proposed scheme is evaluated analytically while simulations performed over the IEEE 802.15.3a UWB channel model are provided to support the theoretical results.**

***Index Terms*—Ultra-wideband, UWB, PPM, cooperation, relay, diversity, power allocation, decode-and-forward, DF, performance analysis, cooperative diversity, correlated noise.**

I. Introduction

Impulse-Radio Ultra-Wideband (IR-UWB) communications attracted significant attention as a strong candidate solution for short-range high data-rate applications. The low tolerated transmission levels and the propagation properties of the UWB signals quickly become limiting factors on the system coverage. In this context, spatial diversity constitutes an additional degree of freedom capable of leveraging the performance and extending the coverage of UWB networks. The spatial diversity techniques include localized diversity techniques where multiple antennas are deployed at the transmitter and/or receiver. These techniques were considered in [1], [2] in the context of IR-UWB communications where high diversity and multiplexing gains were demonstrated over the multi-path UWB channels. On the other hand, in cooperative systems, neighboring nodes in a wireless network cooperate with each other to profit from the underlying spatial diversity in a distributed manner. In this case, a signal transmitted from a source to a destination can be overheard by neighboring relays that can further assist in enhancing the quality of signal reception at the destination.

While the literature on cooperation in the narrow-band context is huge and dates back to about a decade [3]–[5], it was only recently that cooperative UWB systems started attracting a growing attention. In [6], [7], the amplify-and-forward (AF) cooperation protocol was extended to the context of IR-UWB transmissions. In particular, different algebraic space-time (ST) code constructions that are suitable for real-valued UWB transmissions were proposed and analyzed. A cooperation strategy that is based on the orthogonal ST codes was proposed in [8] for dual-hop multi-antenna IR-UWB transmissions. An outage probability analysis and a bit-error-rate (BER) analysis showed that the proposed relaying scheme is capable of achieving better coverage over the multi-path UWB channels. A similar strategy that is based on the orthogonal ST codes was considered in [9] in the context of multi-band orthogonal frequency division multiplexing (MB-OFDM) UWB systems. On the other hand, various cooperation strategies that are based on the decode-and-forward (DF) relaying protocol were provided in [10]–[12]. In [10], the pulse repetitions in time-hopping (TH) UWB systems were exploited for decoupling the data streams received at the destination in a simple and efficient way. In [11], the DF protocol was extended to coherent UWB systems with selective-Rake reception and to non-coherent UWB systems that are based on the differential transmitted reference transmissions. In [12], an accurate BER analysis that is based on the characteristic function evaluation was provided over the realistic IEEE 802.15.4a channel model. Finally, addressing DF relaying with MB-OFDM-UWB systems, the error performance and power allocation were provided in [13] while an upper-bound on the capacity was derived in [14].

The existing UWB cooperation techniques can be classified into two broad categories. (i): Orthogonal techniques where cooperation is performed over two distinct time slots where in the first slot the message is transmitted from the source to the relays (and in some cases to the destination) and in the second slot the message is retransmitted from the relays to the destination [11]–[13]. Despite their good error performance and simplicity, such schemes are characterized by a data-rate reduction where cooperative systems transmit at half the rate of their equivalent non-cooperative systems [11]–[13]. For example, in [11] the symbol duration is doubled (compared to non-cooperative systems) where the first half of this duration is completely dedicated to the communication between the source and the relay while the second half is dedicated to the relay-destination link. This non-efficient use of the system resources is highly penalizing and constitutes a major drawback that renders these simplistic orthogonal schemes not suitable for real-life applications. (ii): The second category

The author is with the Department of Electrical and Computer Engineering of the Lebanese American University (LAU), Byblos, Lebanon. (e-mail: chadi.abourjeily@lau.edu.lb).

corresponds to non-orthogonal cooperation strategies [6], [7], [9], [10] where appropriate encoding schemes render these cooperative systems capable of transmitting at the same data rate as non-cooperative systems. In particular, all transmissions (whether from the source or the relays) occur in the same TDMA time slot. In such systems, the TDMA slots allocated to the relays are not used for transmitting the information of the source, thus the relays can assist the source even if they have their own data to communicate.

In this paper, we propose a novel cooperation strategy that is suitable for IR-UWB communications with Pulse Position Modulation (PPM). Unlike the existing non-orthogonal schemes that extend over several symbol durations, the proposed scheme takes the structure of the multidimensional PPM constellation into consideration to realize symbol-by-symbol cooperation that is completely limited to one symbol duration. The distinction of the proposed scheme compared to the AF and DF protocols is highlighted in what follows. In AF-relaying, the signals received within all PPM slots are amplified and forwarded to the receiver [6], [7]. In a similar manner, in DF-relaying, the relay makes a decision at the end of each symbol duration after inspecting all the received PPM slots [11], [12]. On the other hand, the proposed scheme inspects the signals received within the PPM slots in a sequential manner where the signal retransmitted by the relay during a certain PPM slot depends only on what was received by this relay during the previous slot. This strategy avoids the joint coding/decoding [6], [7] as well as the half-rate transmissions [11], [12] while maintaining high performance levels and diversity orders at the destination. Moreover, unlike [10], the proposed scheme can be implemented independently from the number of time-hopped UWB pulses used to convey one information symbol; in particular, it can be deployed even in the absence of pulse repetitions. As in [6], [7], [9], [10], the proposed non-orthogonal scheme is limited to one TDMA slot (that is allocated to the source). The above attractive features of the proposed scheme come at the expense of a data-rate reduction by a factor of $\frac{M}{M+1}$ compared to non-cooperative M-PPM systems. However, this ratio is much better than the $1/2$ ratio resulting from the orthogonal schemes; moreover, this data-rate reduction decreases with M and approaches one (i.e. no date-rate reduction) for large values of M. An exact performance analysis of the proposed scheme is provided for 2-PPM while an upper-bound is derived for M-PPM with $M > 2$. Based on the obtained error probability expressions, we propose a suboptimal, yet simple, power allocation strategy that turned out to be very close to the optimal strategy. An attractive feature of the proposed power allocation strategy resides in its capability of achieving the same diversity order as the optimal strategy.

II. System Model and Cooperation Strategy

Consider M-ary PPM where the information is modulated by transmitting an UWB pulse in one of the M available time slots. The cooperation strategy that we propose extends over only one symbol duration that will be denoted by T_s. Denote by $a \in \{1, \ldots, M\}$ the PPM symbol to be communicated. In this case, the signal transmitted by the source (S) during the corresponding symbol duration can be written as:

$$s_{\rm s}(t) = \sqrt{\alpha E_s} w(t - (a-1)\delta) \tag{1}$$

where δ stands for duration of each PPM slot and E_s stands for the signal energy. $w(t)$ is the UWB pulse waveform having a duration T_w and which is normalized to have a unit energy. α stands for the fraction of the energy that is transmitted by S with $0 < \alpha < 1$. In this case, the fraction of the energy transmitted by the relay R will be equal to $1-\alpha$ resulting in a cooperative scheme that transmits the same amount of energy as non-cooperative systems. As will be shown later, the choice of α has a major impact on the achievable performance level. An efficient power allocation strategy that adapts the value of α to the specific channel realization will be discussed in Section IV. Finally, no reference to the TH sequence was made in (1) since the proposed cooperation strategy does not depend on the number of time-hopped pulses used to transmit one information symbol. Equation (1) can be written as:

$$s_{\rm s}(t) = \sqrt{\alpha E_s} \sum_{m=1}^{M} a_m w(t - (m-1)\delta) \tag{2}$$

where $a_m = 1$ for $m = a$ and $a_m = 0$ otherwise. In other words, the transmitted symbol can be represented by the M-dimensional vector $[a_1, \ldots, a_M]$ where only one component of this vector (corresponding to the non-empty slot) is different from zero (and equal to one).

Denote by T_c the maximum delay spread of the UWB channel ($T_c \gg T_w$). We assume that the modulation delay δ satisfies the relation $\delta \geq T_c + T_w$ resulting in no interference (at the receiver side) between the different PPM time slots. In other words, we consider the case of orthogonal PPM where all the multi-path components of the frequency-selective channel arrive within a duration that does not exceed δ. With the above constraint on δ being respected, the symbol duration for non-cooperative systems can be chosen as $T_s = M\delta$ resulting in no inter-symbol-interference. For the proposed cooperative system, and in order to be able to realize cooperation over only one symbol duration, we fix $T_s = (M+1)\delta$ resulting in a data-rate reduction of $\frac{M}{M+1}$ compared to non-cooperative systems. This data-rate reduction is transformed into an additional power penalty imposed on the cooperative scheme in all the results that we present in this paper. This choice of T_s will be justified later.

In what follows, we denote by $g_{\rm sd}(t)$, $g_{\rm sr}(t)$ and $g_{\rm rd}(t)$ the convolutions of $w(t)$ with the impulse responses of the channels between S-D, S-R and R-D, respectively. We also assume the presence of a perfect channel estimator that provides R (resp. D) with the value of $g_{\rm sr}(t)$ (resp. $g_{\rm sd}(t)$ and $g_{\rm rd}(t)$) over an integration duration T_i. Evidently, the complexity of these estimators increases with T_i.

When the signal given in (2) is transmitted by S, the signal received at R can be written as:

$$r_{\rm r}(t) = \sqrt{\alpha \beta_{\rm sr} E_s} \sum_{m=1}^{M} a_m g_{\rm sr}(t - (m-1)\delta) + n_{\rm r}(t) \tag{3}$$

where $n_{\rm r}(t)$ stands for the noise that is assumed to be an additive white Gaussian noise (AWGN) with variance $\frac{N_0}{2}$

where N_0 stands for the noise power spectral density. Denote by d_{sd} and d_{sr} the distances from S to D and S to R, respectively. The term β_{sr} in (3) follows from the fact that d_{sr} might be different from d_{sd}. In other words, a signal-to-noise ratio (SNR) of $\frac{E_s}{N_0}$ at D will be equivalent to a SNR of $\beta_{\text{sr}}\frac{E_s}{N_0}$ at R. Performing a typical link power budget analysis shows that $\beta_{\text{sr}} = \left(\frac{d_{\text{sd}}}{d_{\text{sr}}}\right)^2$ assuming that the received power decreases with the square of the distance.

The role of R will be based on the following decision variables that will be evaluated in a sequential manner starting from $m = 1$ and ending by $m = M$:

$$y_{\text{r}}^{(m)} = \int_0^{T_i} r_{\text{r}}(t) g_{\text{sr}}(t - (m-1)\delta) \text{d}t \tag{4}$$

where T_i stands for the integration time. In the above equation, it is assumed that R has acquired the value of the function $g_{\text{sr}}(t)$ over a duration T_i via a channel estimation process that is assumed to be perfect in what follows. Evidently, the complexity of this estimator increases with T_i. Following from the orthogonality of the PPM signal set, (4) reduces to:

$$y_{\text{r}}^{(m)} = \sqrt{\alpha\beta_{\text{sr}}E_s} h_{\text{sr}} a_m + n_{\text{r}}^{(m)} \tag{5}$$

where $h_{\text{sr}} \triangleq \int_0^{T_i} g_{\text{sr}}^2(t)\text{d}t$ stands for the channel energy captured along the link S-R over a duration T_i. In the same way, $n_{\text{r}}^{(m)} = \int_0^{T_i} n_{\text{r}}(t) g_{\text{sr}}(t-(m-1)\delta)\text{d}t$ is a Gaussian random variable with variance $h_{\text{sr}}N_0/2$. Note that the noise terms $n_{\text{r}}^{(1)}, \ldots, n_{\text{r}}^{(M)}$ are uncorrelated.

The cooperation strategy at R is as follows. First, R observes the received signal over the interval $[0 \quad \delta]$ to evaluate the decision variable $y_{\text{r}}^{(1)}$. R then compares $y_{\text{r}}^{(1)}$ with a ceratin threshold level I_{th}. If $y_{\text{r}}^{(1)} \geq I_{th}$, then R will retransmit an UWB pulse in the next PPM slot (which is the second slot) and it will wait for the next symbol; otherwise, the relay will not retransmit any pulse and it will start inspecting the received signal over the next interval $[\delta \quad 2\delta]$. This operation will be repeated in a sequential manner starting from the first PPM slot and ending with the M-th slot. In other words, for the m-th slot, R evaluates $y_{\text{r}}^{(m)}$ and compares it with I_{th}. If $y_{\text{r}}^{(m)} \geq I_{th}$, then R retransmits a pulse in slot $m+1$; otherwise it restarts the same operation with $m+1$. Note that whenever the relation $y_{\text{r}}^{(m)} \geq I_{th}$ is satisfied for a ceratin value of m, the remaining decision variables $y_{\text{r}}^{(m+1)}, \ldots, y_{\text{r}}^{(M)}$ will not be evaluated. Note that m is incremented sequentially from 1 to M and that this sequential analysis ensures the causality at R. Consider the case where $y_{\text{r}}^{(1)}, \ldots, y_{\text{r}}^{(M-1)}$ are all smaller than I_{th} while $y_{\text{r}}^{(M)} \geq I_{th}$. This case necessitates the retransmission of a pulse in the $(M+1)$-th slot implying that the symbol duration has to be increased from $T_s = M\delta$ (for non-cooperative systems) to $T_s = (M+1)\delta$. Note that the relay is left with a duration of $\delta - T_i$ to further process the decision variable $y_{\text{r}}^{(m)}$ that was collected over a duration T_i. Given that T_i is often chosen to take small values in order to reduce the receiver complexity while δ takes large values in order to eliminate interference, this duration is sufficient to encompass all processing delays. In what follows, I_{th} is chosen as: $I_{th} = \sqrt{\alpha\beta_{\text{sr}}E_s}h_{\text{sr}}/2$. In other words, the threshold level is fixed midway between the maximum noiseless signal level ($\max[y_{\text{r}}^{(m)}] = \sqrt{\alpha\beta_{\text{sr}}E_s}h_{\text{sr}}$) and the minimum noiseless signal level ($\min[y_{\text{r}}^{(m)}] = 0$). Note that since the noise is AWGN, this value of I_{th} minimizes the error probability along the S-R link.

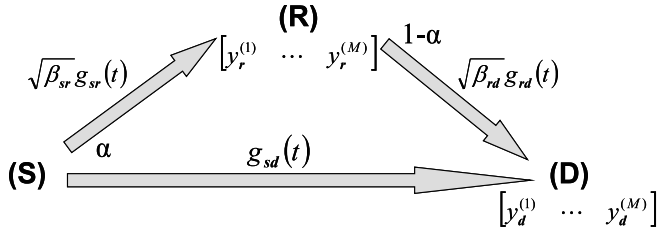

Fig. 1. Parameters of the cooperative system.

Denote by $\hat{m}$ the smallest integer in the set $\{1, \ldots, M\}$ for which $y_{\text{r}}^{(\hat{m})} \geq I_{th}$ and construct the vector $[\hat{a}_1, \ldots, \hat{a}_M]$ such that $\hat{a}_m = 1$ for $m = \hat{m}$ and $\hat{a}_m = 0$ otherwise. In this case, the signal transmitted by R can be written as:

$$s_{\text{r}}(t) = \sqrt{(1-\alpha)E_s} \sum_{m=1}^{M} \hat{a}_m w(t - m\delta) \tag{6}$$

where unlike (2) in which $w(t)$ was shifted by $(m-1)\delta$, $w(t)$ is now shifted by $m\delta$.

Now, the signal received at D can be written as:

$$\begin{aligned} r_{\text{d}}(t) = &\sqrt{\alpha E_s} \sum_{m=1}^{M} a_m g_{\text{sd}}(t - (m-1)\delta) \\ &+ \sqrt{(1-\alpha)\beta_{\text{rd}}E_s} \sum_{m=1}^{M} \hat{a}_m g_{\text{rd}}(t - m\delta) + n_{\text{d}}(t) \end{aligned} \tag{7}$$

where, as in (3), $\beta_{\text{rd}} = \left(\frac{d_{\text{sd}}}{d_{\text{rd}}}\right)^2$ and $n_{\text{d}}(t)$ is the white Gaussian noise with variance $N_0/2$.

A bank of correlators is deployed at D in order to collect the following M decision variables (for $m = 1, \ldots, M$):

$$y_{\text{d}}^{(m)} = \int_0^{T_i} r_{\text{d}}(t) \left[g_{\text{sd}}(t - (m-1)\delta) + g_{\text{rd}}(t - m\delta)\right] \text{d}t \tag{8}$$

Following from (7), equation (8) simplifies to:

$$\begin{aligned} y_{\text{d}}^{(m)} = &\sqrt{\alpha E_s} h_{\text{sd}} a_m + \sqrt{(1-\alpha)\beta_{\text{rd}}E_s} h_{\text{rd}} \hat{a}_m \\ &+ \left[\sqrt{\alpha E_s} a_{m+1} + \sqrt{(1-\alpha)\beta_{\text{rd}}E_s}\hat{a}_{m-1}\right] h_{\text{in}} + n_{\text{d}}^{(m)} \end{aligned} \tag{9}$$

where $h_{\text{sd}} \triangleq \int_0^{T_i} g_{\text{sd}}^2(t)\text{d}t$, $h_{\text{rd}} \triangleq \int_0^{T_i} g_{\text{rd}}^2(t)\text{d}t$ and $h_{\text{in}} \triangleq \int_0^{T_i} g_{\text{sd}}(t) g_{\text{rd}}(t)\text{d}t$. We also set: $a_{M+1} \triangleq 0$ and $\hat{a}_0 \triangleq 0$. The noise terms are given by: $n_{\text{d}}^{(m)} = \int_0^{T_i} n_{\text{d}}(t) \left[g_{\text{sd}}(t - (m-1)\delta) + g_{\text{rd}}(t - m\delta)\right] \text{d}t$. It can be proven that:

$$\text{E}\left[n_{\text{d}}^{(m)} n_{\text{d}}^{(m')}\right] = \frac{N_0}{2} \begin{cases} h_{\text{sd}} + h_{\text{rd}}, & m = m'; \\ \sqrt{h_{\text{sd}}h_{\text{rd}}}, & |m - m'| = 1; \\ 0, & \text{otherwise.} \end{cases} \tag{10}$$

where E[.] stands for the averaging operator. Equation (10) shows that the noise terms corresponding to two consecutive PPM slots are correlated. The different parameters of the system under consideration are depicted in Fig. 1.

III. Performance Analysis

In this section, we will evaluate the performance of the proposed scheme in terms of the achievable conditional symbol error probability. At a first time, we consider the case of $M=2$ and then extend the results to the case of $M>2$.

A numerical analysis performed over the IEEE 802.15.3a channel model [15] showed that the interference term h_{in} takes very small values and, hence, can be neglected. This can be justified by the randomness of the polarity of the multi-path components corresponding to $g_{\text{sd}}(t)$ and $g_{\text{rd}}(t)$. Consequently, in this section we evaluate the performance assuming that $h_{\text{in}}=0$. This assumption will be further supported by the numerical results in Section V. For the sake of simplicity, we set $h_1=\sqrt{\alpha\beta_{\text{sr}}E_s}h_{\text{sr}}$, $h_2=\sqrt{\alpha E_s}h_{\text{sd}}$ and $h_3=\sqrt{(1-\alpha)\beta_{\text{rd}}E_s}h_{\text{rd}}$ in what follows. The channel state is defined by: $H=[h_{\text{sr}},h_{\text{sd}},h_{\text{rd}}]$.

Consider the case $M=2$. Given that the noise terms $n_{\text{d}}^{(1)}$ and $n_{\text{d}}^{(2)}$ are correlated Gaussian random variables (r.v.s), we first apply the following transformation that will simplify the error analysis:

$$\begin{bmatrix} u \\ v \end{bmatrix} = \frac{1}{\sqrt{2}} \begin{bmatrix} 1 & 1 \\ 1 & -1 \end{bmatrix} \begin{bmatrix} n_{\text{d}}^{(1)} \\ n_{\text{d}}^{(2)} \end{bmatrix} \tag{11}$$

This transformation results in the zero-mean independent Gaussian r.v.s u and v whose variances are given by:

$$\sigma_u^2 = \left(h_{\text{sd}}+h_{\text{rd}}+\sqrt{h_{\text{sd}}h_{\text{rd}}}\right)N_0/2 \tag{12}$$

$$\sigma_v^2 = \left(h_{\text{sd}}+h_{\text{rd}}-\sqrt{h_{\text{sd}}h_{\text{rd}}}\right)N_0/2 \tag{13}$$

Assume first that the PPM symbol $m=1$ was transmitted. In this case, the decision variables at the relay are given by: $y_{\text{r}}^{(1)}=h_1+n_{\text{r}}^{(1)}$ and $y_{\text{r}}^{(2)}=n_{\text{r}}^{(2)}$. Three cases are possible at R. Case (i.1): $y_{\text{r}}^{(1)}\geq I_{th}$ implying that the symbol $\hat{m}=1$ will be retransmitted (in the second slot). Case (i.2): $y_{\text{r}}^{(1)}<I_{th}$ and $y_{\text{r}}^{(2)}\geq I_{th}$ implying that the symbol $\hat{m}=2$ will be retransmitted (in the third added slot). Case (i.3): $y_{\text{r}}^{(1)}<I_{th}$ and $y_{\text{r}}^{(2)}<I_{th}$ implying that no symbol will be retransmitted by R. Given that $I_{th}=h_1/2$ and $(n_{\text{r}}^{(1)},n_{\text{r}}^{(2)})$ are uncorrelated Gaussian r.v.s with variances $h_{\text{sr}}N_0/2$, then it is straightforward to prove that:

$$\Pr(h_1+n_{\text{r}}^{(1)}<I_{th})=1-\Pr(h_1+n_{\text{r}}^{(1)}\geq I_{th})=p \tag{14}$$

$$\Pr(n_{\text{r}}^{(2)}\geq I_{th})=1-\Pr(n_{\text{r}}^{(2)}<I_{th})=p \tag{15}$$

where the probability p is given by:

$$p=Q\left(\frac{h_1/2}{\sqrt{h_{\text{sr}}N_0/2}}\right)=Q\left(\sqrt{\frac{\alpha\beta_{\text{sr}}h_{\text{sr}}E_s}{2N_0}}\right) \tag{16}$$

where the function $Q(x)$ is defined as: $Q(x)=\frac{1}{\sqrt{2\pi}}\int_x^\infty e^{-t^2/2}\text{d}t$.

Case (i.1) occurs with probability $1-p$ following from (14). Given that $\hat{m}=1$, then ignoring h_{in} in (9) results in the following decision variables at D: $y_{\text{d}}^{(1)}=h_2+h_3+n_{\text{d}}^{(1)}$ and $y_{\text{d}}^{(2)}=n_{\text{d}}^{(2)}$. Given that the symbol $m=1$ was transmitted, then the error probability at D can be written as:

$$P_1 \triangleq \Pr(h_2+h_3+n_{\text{d}}^{(1)}<n_{\text{d}}^{(2)}) \tag{17}$$

$$=\int_{-\infty}^{+\infty}\int_{-\infty}^{n_{\text{d}}^{(2)}-h_2-h_3} p(n_{\text{d}}^{(1)},n_{\text{d}}^{(2)})\text{d}n_{\text{d}}^{(1)}\text{d}n_{\text{d}}^{(2)} \tag{18}$$

where $p(n_{\text{d}}^{(1)},n_{\text{d}}^{(2)})$ stands for the joint probability density function of the correlated Gaussian r.v.s $n_{\text{d}}^{(1)}$ and $n_{\text{d}}^{(2)}$:

$$p(x,y)=\frac{1}{2\pi\sigma_n^2\sqrt{1-\rho^2}}\exp\left(\frac{-x^2+2\rho xy-y^2}{2\sigma_n^2(1-\rho^2)}\right) \tag{19}$$

where, from (10), $\sigma_n^2=\frac{N_0}{2}(h_{\text{sd}}+h_{\text{rd}})$ and $\rho=\frac{\sqrt{h_{\text{sd}}h_{\text{rd}}}}{h_{\text{sd}}+h_{\text{rd}}}$.

Applying the transformation given in (11), the integral in (18) simplifies to:

$$P_1=\int_{-\infty}^{+\infty}p(u)\text{d}u\int_{-\infty}^{-\frac{h_2+h_3}{\sqrt{2}}}p(v)\text{d}v \tag{20}$$

$$=1\times Q\left(\frac{h_2+h_3}{\sqrt{2\sigma_v^2}}\right)=Q\left(\frac{\sqrt{\alpha}h_{\text{sd}}+\sqrt{(1-\alpha)\beta_{\text{rd}}}h_{\text{rd}}}{\sqrt{h_{\text{sd}}+h_{\text{rd}}-\sqrt{h_{\text{sd}}h_{\text{rd}}}}}\sqrt{\frac{E_s}{N_0}}\right) \tag{21}$$

where $p(u)$ and $p(v)$ stand for the probability density functions of the r.v.s u and v defined in (11). The equivalence between the integrals in (18) and (20) is better illustrated in Fig. 2.

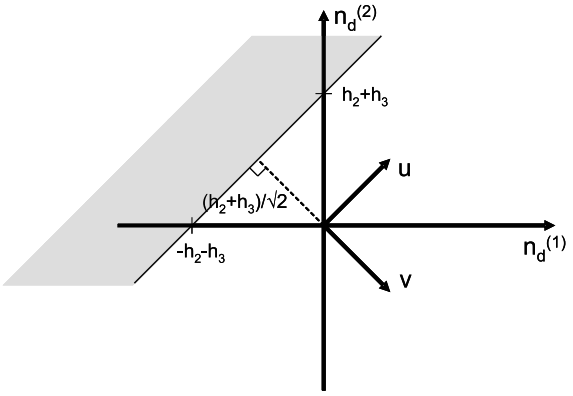

Fig. 2. The bivariate Gaussian vector $(n_{\text{d}}^{(1)},n_{\text{d}}^{(2)})$, the r.v.s u and v and the integration area corresponding to equations (18) and (20).

Case (i.2) occurs with probability p^2 following from (14) and (15). In this case, $\hat{m}=2$ resulting in the following decision variables: $y_{\text{d}}^{(1)}=h_2+n_{\text{d}}^{(1)}$ and $y_{\text{d}}^{(2)}=h_3+n_{\text{d}}^{(2)}$. Following an analysis similar to that presented in equations (17)-(21) where h_2+h_3 is now replaced by h_2-h_3, we obtain the following expression of the probability of error in case (i.2):

$$P_2=Q\left(\frac{\sqrt{\alpha}h_{\text{sd}}-\sqrt{(1-\alpha)\beta_{\text{rd}}}h_{\text{rd}}}{\sqrt{h_{\text{sd}}+h_{\text{rd}}-\sqrt{h_{\text{sd}}h_{\text{rd}}}}}\sqrt{\frac{E_s}{N_0}}\right) \tag{22}$$

Case (i.3) occurs with probability $p(1-p)$. In this case, no symbol is retransmitted by R resulting in the following decision variables at D: $y_{\text{d}}^{(1)}=h_2+n_{\text{d}}^{(1)}$ and $y_{\text{d}}^{(2)}=n_{\text{d}}^{(2)}$. Replacing h_2+h_3 by h_2 in (21) results in the following expression of the probability of error in case (i.3):

$$P_3=Q\left(\frac{\sqrt{\alpha}h_{\text{sd}}}{\sqrt{h_{\text{sd}}+h_{\text{rd}}-\sqrt{h_{\text{sd}}h_{\text{rd}}}}}\sqrt{\frac{E_s}{N_0}}\right) \tag{23}$$

Evaluating the weighted sum of the probabilities in equations (21)-(23) results in:

$$P_{e|H}^{(1)} = (1-p)P_1 + p^2 P_2 + p(1-p)P_3 \tag{24}$$

where $P_{e|H}^{(1)}$ stands for the conditional error probability when the symbol $m=1$ is transmitted.

Assume now that the symbol $m=2$ is transmitted. In this case, the decision variables at R are given by: $y_{\text{r}}^{(1)} = n_{\text{r}}^{(1)}$ and $y_{\text{r}}^{(2)} = h_1 + n_{\text{r}}^{(2)}$. Three cases are possible at D as follows.

Case (ii.1): $y_{\text{r}}^{(1)} \geq I_{th}$ occurring with probability p. In this case, $\hat{m}=1$ and the decision variables at D are: $y_{\text{d}}^{(1)} = h_3 + n_{\text{d}}^{(1)}$ and $y_{\text{d}}^{(2)} = h_2 + n_{\text{d}}^{(2)}$. Given the analogy between cases (ii.1) and (i.2), then the conditional error probability in this case is equal to P_2 given in (22).

Case (ii.2): $y_{\text{r}}^{(1)} < I_{th}$ and $y_{\text{r}}^{(2)} \geq I_{th}$ occurring with probability $(1-p)^2$. In this case, $\hat{m}=2$ resulting in $y_{\text{d}}^{(1)} = n_{\text{d}}^{(1)}$ and $y_{\text{d}}^{(2)} = h_2 + h_3 + n_{\text{d}}^{(2)}$. Given the analogy between cases (ii.2) and (i.1), then the conditional error probability in this case is equal to P_1 given in (21).

Case (ii.3): $y_{\text{r}}^{(1)} < I_{th}$ and $y_{\text{r}}^{(2)} < I_{th}$ occurring with probability $(1-p)p$. In this case: $y_{\text{d}}^{(1)} = n_{\text{d}}^{(1)}$ and $y_{\text{d}}^{(2)} = h_2 + n_{\text{d}}^{(2)}$ resulting in an error probability that is equal to P_3 given in (23). Finally, combining the above cases results in:

$$P_{e|H}^{(2)} = pP_2 + (1-p)^2 P_1 + p(1-p)P_3 \tag{25}$$

where $P_{e|H}^{(2)}$ stands for the conditional error probability when the symbol $m=2$ is transmitted.

Finally, combining equations (24) and (25) results in the following expression of the conditional symbol error probability (SEP):

$$P_{e|H} = \frac{1}{2}\left[P_{e|H}^{(1)} + P_{e|H}^{(2)}\right] \tag{26}$$

Equations (24) and (25) show a rather surprising result where the error probabilities on the two symbols of the binary PPM constellation are not the same. In other words, despite the symmetry of the PPM signal set, the probability of making an error depends on which symbol was transmitted showing that this symmetry is broken by the structure of the proposed cooperation strategy. In a more precise manner, subtracting (24) from (25) shows that: $P_{e|H}^{(2)} - P_{e|H}^{(1)} = p(1-p)[P_2 - P_1]$. On the other hand, given that $\sqrt{\alpha}h_{\text{sd}} + \sqrt{(1-\alpha)\beta_{\text{rd}}}h_{\text{rd}} \geq \sqrt{\alpha}h_{\text{sd}} - \sqrt{(1-\alpha)\beta_{\text{rd}}}h_{\text{rd}}$ (since all involved quantities are positive), then $P_1 \leq P_2$ following from (21)-(22). This results in $P_{e|H}^{(2)} \geq P_{e|H}^{(1)}$ showing that it is more probable to make errors on the second PPM symbol $m=2$. This follows from the proposed cooperation strategy where, whenever one decision variable at R exceeds threshold, the subsequent decision variables will be ignored (i.e. not compared with the threshold). In fact, for the symbol $m=1$ the first slot contains a signal energy, then with high probability the second slot (containing only noise) will not be considered. On the other hand, for the symbol $m=2$ the first slot contains only noise, then with high probability the second slot (containing a signal energy) will be considered. In other words, the retransmission of the correct symbol by R for $m=1$ is based on one noisy slot (containing also a signal) while this correct retransmission for $m=2$ is based on two noisy slots (where only one of them contains a signal). This justifies the fact that the symbol $m=1$ will be reconstructed with a higher fidelity.

Note that the integrals in (18) and (20) must be performed over integration regions in a M-dimensional space. Consequently, for $M > 2$, these integrals are difficult to solve rendering an exact expression of the conditional SEP difficult to obtain in this case. Therefore, we resort to bounding techniques that allow us to obtain the following result.

Proposition: For M-ary PPM constellations with $M > 2$, the conditional SEP of the proposed cooperation scheme can be upper-bounded by:

$$P_{e|H} = \frac{1}{M}\sum_{m=1}^{M} P_{e|H}^{(m)} = \frac{1}{M}\sum_{m=1}^{M}\sum_{i=1}^{M+1} p_i^{(m)} P_i^{(m)} \tag{27}$$

$$\leq \frac{1}{M}\sum_{m=1}^{M}\sum_{i=1}^{M+1} p_i^{(m)} \sum_{j=1\ ;\ j\neq m}^{M} P_{i,j}^{(m)} \tag{28}$$

where the probability $P_{i,j}^{(m)}$ is given by:

$$P_{i,j}^{(m)} = Q\left(\frac{\sqrt{\alpha}h_{\text{sd}} + (\delta_{m,i} - \delta_{j,i})\sqrt{(1-\alpha)\beta_{\text{rd}}}h_{\text{rd}}}{\sqrt{h_{\text{sd}} + h_{\text{rd}} - (\delta_{j,m-1} + \delta_{j,m+1})\sqrt{h_{\text{sd}}h_{\text{rd}}}}}\sqrt{\frac{E_s}{N_0}}\right) \tag{29}$$

where $\delta_{i,j} = 1$ for $i = j$ and $\delta_{i,j} = 0$ for $i \neq j$. The probability $p_i^{(m)}$ can be written as:

$$p_i^{(m)} = \begin{cases} (1-p)^{i-1}p, & i < m; \\ (1-p)^i, & i = m; \\ (1-p)^{i-2}p^2, & m < i \leq M; \\ (1-p)^{i-2}p, & i = M+1. \end{cases} \tag{30}$$

where the probability p is given in (16).

Proof: The proof is provided in the appendix.

Note that, as in the case of $M=2$, the error probability is not the same for all M-PPM symbols in the case of $M > 2$. As shown in the appendix, the upper-bound in (28) follows from the union bound. Consequently, (28) becomes close to the exact value of $P_{e|H}$ for large values of the SNR; i.e. in the range of SNRs where cooperative diversity is useful.

Finally, since the conditional error probabilities in equations (24),(25) and (28) do not lend themselves to a simple analytical integration over the IEEE 802.15.3a channel model, then we evaluate the SEP according to:

$$P_e = \frac{1}{M}\sum_{m=1}^{M} P_e^{(m)} \tag{31}$$

where the average probabilities $\{P_e^{(m)}\}_{m=1}^{M}$ are obtained by numerically integrating $\{P_{e|H}^{(m)}\}_{m=1}^{M}$.

IV. Power Allocation

It is desirable to derive the optimal value of α that minimizes the conditional symbol error probability given in (26) and (28) for $M=2$ and $M>2$, respectively. However, a closed-form solution is not possible and, instead, we adopt a suboptimal approach based on minimizing two upper-bounds on the asymptotic values of (26) and (28). As a first step, we

will perform the derivation with $M = 2$ and then consider the case of $M > 2$. The corresponding value of α is found to be dependent on the SNR and channel state.

For $M = 2$, from (24), (25) and (26), the conditional SEP can be approximated by the following expression for large values of the SNR:

$$P_{e|H} \approx \frac{1}{2}\left[2P_1 + pP_2 + 2pP_3\right] \tag{32}$$

where this equation follows from approximating (24) and (25) for $p \ll 1$.

From (22) and (23), we observe that $P_3 \leq P_2$ implying that (32) can be upper-bounded by:

$$P_{e|H} \leq \frac{1}{2}\left[2P_1 + 3pP_2\right] \leq \frac{3}{2}\left[P_1 + pP_2\right] \leq 3\max\{P_1, pP_2\} \tag{33}$$

The suboptimal approach that we adopt corresponds to determining the value of α that minimizes $\max\{P_1, pP_2\}$. For simplicity, from (16), (21) and (22), we write P_1 and pP_2 as:

$$f_1(\alpha) \triangleq P_1 = Q\left(k(\sqrt{\alpha}h_{\text{sd}} + \sqrt{(1-\alpha)\beta_{\text{rd}}}h_{\text{rd}})\right) \tag{34}$$

$$f_2(\alpha) \triangleq pP_2 = Q\left(k_1\sqrt{\alpha}\right) Q\left(k(\sqrt{\alpha}h_{\text{sd}} - \sqrt{(1-\alpha)\beta_{\text{rd}}}h_{\text{rd}})\right) \tag{35}$$

where k and k_1 are two constants that do not depend on α:

$$k \triangleq \sqrt{\frac{E_s}{N_0(h_{\text{sd}} + h_{\text{rd}} - \sqrt{h_{\text{sd}}h_{\text{rd}}})}} \quad ; \quad k_1 \triangleq \sqrt{\frac{\beta_{\text{sr}}h_{\text{sr}}E_s}{2N_0}} \tag{36}$$

Note that the term pP_2 can not be neglected compared to P_1. In fact, $k(\sqrt{\alpha}h_{\text{sd}} + \sqrt{(1-\alpha)\beta_{\text{rd}}}h_{\text{rd}})$ and $k_1\sqrt{\alpha}$ are always positive implying, from (34) and (35), that P_1 and p decrease rapidly with the SNR. On the other hand, the term $k(\sqrt{\alpha}h_{\text{sd}} - \sqrt{(1-\alpha)\beta_{\text{rd}}}h_{\text{rd}})$ is small in absolute value (since it corresponds to the difference between two comparable positive numbers) and it can be positive or negative implying, from (35), that P_2 can take large values even for large SNRs. As a conclusion, P_2 is several orders of magnitudes larger than p and P_1 implying that P_1 and pP_2 have comparable values.

We define α_1 as the value of α that minimizes the function $f_1(\alpha)$ given in (34). It can be easily proven that α_1 takes the following value:

$$\alpha_1 = \frac{h_{\text{sd}}^2}{h_{\text{sd}}^2 + \beta_{\text{rd}}h_{\text{rd}}^2} \tag{37}$$

where the last equation shows that $0 \leq \alpha_1 \leq 1$.

Over the interval $[0 \quad \alpha_1]$, the function $f_1(\alpha)$ decreases from $f_1(0) = Q(k\sqrt{\beta_{\text{rd}}}h_{\text{rd}})$ to $f_1(\alpha_1) = Q(k\sqrt{h_{\text{sd}}^2 + \beta_{\text{rd}}h_{\text{rd}}^2})$ and over the interval $[\alpha_1 \quad 1]$ $f_1(\alpha)$ increases from $f_1(\alpha_1)$ to $f_1(1) = Q(kh_{\text{sd}})$. On the other hand, the function $f_2(\alpha)$ is strictly decreasing for $\alpha \in [0 \quad 1]$ where it decreases from $f_2(0) = \frac{1}{2}Q(-k\sqrt{\beta_{\text{rd}}}h_{\text{rd}}) = \frac{1}{2}[1 - Q(k\sqrt{\beta_{\text{rd}}}h_{\text{rd}})]$ to $f_2(1) = Q(k_1)Q(kh_{\text{sd}})$. Note that $f_2(\alpha)$ varies faster than $f_1(\alpha)$ and that $Q(k_1)Q(kh_{\text{sd}}) \leq Q(kh_{\text{sd}})$ implying that $f_2(1) \leq f_1(1)$. Consequently, two cases are possible.

Case 1: $\frac{1}{2}Q(-k\sqrt{\beta_{\text{rd}}}h_{\text{rd}}) \leq Q(k\sqrt{\beta_{\text{rd}}}h_{\text{rd}})$ implying that $Q(k\sqrt{\beta_{\text{rd}}}h_{\text{rd}}) \geq \frac{1}{3}$ or $k\sqrt{\beta_{\text{rd}}}h_{\text{rd}} \leq Q^{-1}\left(\frac{1}{3}\right)$. In this case, $f_2(0) \leq f_1(0)$. Moreover, since $f_2(1) \leq f_1(1)$ and $f_2(\alpha)$ varies faster than $f_1(\alpha)$, then $f_2(\alpha)$ is always below $f_1(\alpha)$ implying that $\max\{P_1, pP_2\} = f_1(\alpha)$. In this case, the value of α that minimizes $\max\{P_1, pP_2\}$ is $\alpha = \alpha_1$ that minimizes $f_1(\alpha)$.

Case 2: $k\sqrt{\beta_{\text{rd}}}h_{\text{rd}} > Q^{-1}\left(\frac{1}{3}\right)$. In this case $f_2(0) > f_1(0)$. Moreover, since $f_2(1) \leq f_1(1)$, then the functions $f_1(\alpha)$ and $f_2(\alpha)$ intersect in one point implying that $\max\{P_1, pP_2\}$ is minimized at this point. In fact, for any other point, we have either $f_1(\alpha) > f_2(\alpha)$ or $f_2(\alpha) > f_1(\alpha)$ implying that $\max\{f_1(\alpha), f_2(\alpha)\}$ will increase. In other words, the upper-bound in (33) is minimized for the value of α that is the solution of the equation: $f_1(\alpha) = f_2(\alpha)$.

As a conclusion, the suboptimal power allocation strategy that we propose is given by:

$$\alpha = \begin{cases} \frac{h_{\text{sd}}^2}{h_{\text{sd}}^2 + \beta_{\text{rd}}h_{\text{rd}}^2}, & k\sqrt{\beta_{\text{rd}}}h_{\text{rd}} \leq Q^{-1}\left(\frac{1}{3}\right); \\ \alpha \mid f_1(\alpha) = f_2(\alpha), & k\sqrt{\beta_{\text{rd}}}h_{\text{rd}} > Q^{-1}\left(\frac{1}{3}\right). \end{cases} \tag{38}$$

where the equation $f_1(\alpha) = f_2(\alpha)$ has to be solved numerically.

Note that since k increases with the SNR, then case 1 is more easily satisfied for small SNRs while case 2 holds for large values of the SNR. In this case, the solution of $f_1(\alpha) = f_2(\alpha)$ can be obtained analytically by approximating $Q(x)$ by $e^{-x^2/2}$ where this approximation becomes more accurate for larger values of the SNR. It is straight-forward to prove that this solution (that is always in the interval $[0 \quad 1]$) is given by:

$$\alpha = \frac{16k^4\beta_{\text{rd}}h_{\text{sd}}^2h_{\text{rd}}^2}{16k^4\beta_{\text{rd}}h_{\text{sd}}^2h_{\text{rd}}^2 + k_1^4} \tag{39}$$

We next consider the case $M > 2$. We first derive an upper-bound on the conditional SEP assuming that the transmitted symbols are reconstructed at the relay with a sufficiently high fidelity ($p \ll 1$).

We next separate the four cases given in (30). (i): For $i < m$, $p_i^{(m)} \approx p$ from (30). On the other hand, in (29), $\delta_{m,i} = 0$ while $\delta_{j,i}$ and $(\delta_{j,m-1} + \delta_{j,m+1})$ can be either 0 or 1. Consequently, the summation in (28) contains terms of the form $pQ\left(k\sqrt{\alpha}h_{\text{sd}}\right)$, $pQ\left(k'\sqrt{\alpha}h_{\text{sd}}\right)$, $pQ\left(k(\sqrt{\alpha}h_{\text{sd}} - \sqrt{(1-\alpha)\beta_{\text{rd}}}h_{\text{rd}})\right)$ and $pQ\left(k'(\sqrt{\alpha}h_{\text{sd}} - \sqrt{(1-\alpha)\beta_{\text{rd}}}h_{\text{rd}})\right)$ where the constant k is defined in (36) while the constant k' (that does not depend on α) is given by:

$$k' \triangleq \sqrt{\frac{E_s}{N_0(h_{\text{sd}} + h_{\text{rd}})}} \tag{40}$$

(ii): For $i = m$, $p_i^{(m)} \approx 1$ from (30). In this case, $\delta_{m,i} = 1$, $\delta_{j,i} = 0$ (since $j \neq m = i$) while $(\delta_{j,m-1} + \delta_{j,m+1})$ can be either 0 or 1. Consequently, the summation in (28) contains terms of the form $Q\left(k(\sqrt{\alpha}h_{\text{sd}} + \sqrt{(1-\alpha)\beta_{\text{rd}}}h_{\text{rd}})\right)$ and $Q\left(k'(\sqrt{\alpha}h_{\text{sd}} + \sqrt{(1-\alpha)\beta_{\text{rd}}}h_{\text{rd}})\right)$. (iii): For $m < i \leq M$, $p_i^{(m)} \approx 0$ from (30) implying that the corresponding terms can be neglected in (28). (iv): For $i = M+1$, $p_i^{(m)} \approx p$ from (30). In this case, $\delta_{m,i} = 0$ (since $m \in \{1, \ldots, M\}$ while $i = M+1$), $\delta_{j,i} = 0$ (since $j \in \{1, \ldots, m-1, m+1, \ldots, M\}$) while $(\delta_{j,m-1} + \delta_{j,m+1})$ can be either 0 or 1. Consequently, the summation in (28) contains terms of the form $pQ\left(k\sqrt{\alpha}h_{\text{sd}}\right)$ and $pQ\left(k'\sqrt{\alpha}h_{\text{sd}}\right)$.

Consequently, for $p \ll 1$, (28) can be approximated by:

$$P_{e|H} \approx \frac{1}{M}\left[n_1 pQ\left(k\sqrt{\alpha}h_{\text{sd}}\right) + n_2 pQ\left(k'\sqrt{\alpha}h_{\text{sd}}\right) + n_3 pQ\left(k(\sqrt{\alpha}h_{\text{sd}} - \sqrt{(1-\alpha)\beta_{\text{rd}}}h_{\text{rd}})\right) + n_4 pQ\left(k'(\sqrt{\alpha}h_{\text{sd}} - \sqrt{(1-\alpha)\beta_{\text{rd}}}h_{\text{rd}})\right) + n_5 Q\left(k(\sqrt{\alpha}h_{\text{sd}} + \sqrt{(1-\alpha)\beta_{\text{rd}}}h_{\text{rd}})\right) + n_6 Q\left(k'(\sqrt{\alpha}h_{\text{sd}} + \sqrt{(1-\alpha)\beta_{\text{rd}}}h_{\text{rd}})\right)\right] \quad (41)$$

where $n_1, \ldots, n_6$ correspond to the number of times that the corresponding probability terms appear in $P_{e|H}$.

From (36) and (40), we observe that $k \geq k'$ implying that (41) can be upper-bounded by:

$$P_{e|H} \leq \frac{1}{M}\left[(n_1+n_2)pQ\left(k'\sqrt{\alpha}h_{\text{sd}}\right) + (n_3+n_4)pQ\left(k'(\sqrt{\alpha}h_{\text{sd}} - \sqrt{(1-\alpha)\beta_{\text{rd}}}h_{\text{rd}})\right) + (n_5+n_6)Q\left(k'(\sqrt{\alpha}h_{\text{sd}} + \sqrt{(1-\alpha)\beta_{\text{rd}}}h_{\text{rd}})\right)\right] \quad (42)$$

Since $k'\sqrt{\alpha}h_{\text{sd}} \geq k'(\sqrt{\alpha}h_{\text{sd}} - \sqrt{(1-\alpha)\beta_{\text{rd}}}h_{\text{rd}})$, then:

$$P_{e|H} \leq \frac{1}{M}\left[(n_5+n_6)Q\left(k'(\sqrt{\alpha}h_{\text{sd}} + \sqrt{(1-\alpha)\beta_{\text{rd}}}h_{\text{rd}})\right) + (n_1+n_2+n_3+n_4)pQ\left(k'(\sqrt{\alpha}h_{\text{sd}} - \sqrt{(1-\alpha)\beta_{\text{rd}}}h_{\text{rd}})\right)\right] \quad (43)$$

Defining N as $N \triangleq \max\{(n_1+n_2+n_3+n_4), (n_5+n_6)\}$, then (43) can be upper-bounded by:

$$P_{e|H} \leq \frac{2N}{M}\max\left\{Q\left(k'(\sqrt{\alpha}h_{\text{sd}} + \sqrt{(1-\alpha)\beta_{\text{rd}}}h_{\text{rd}})\right), pQ\left(k'(\sqrt{\alpha}h_{\text{sd}} - \sqrt{(1-\alpha)\beta_{\text{rd}}}h_{\text{rd}})\right)\right\} \quad (44)$$

The approach that we adopt in the case $M > 2$ corresponds to choosing α as the value that minimizes $\max\{f_1'(\alpha), f_2'(\alpha)\}$ where:

$$f_1'(\alpha) = Q\left(k'(\sqrt{\alpha}h_{\text{sd}} + \sqrt{(1-\alpha)\beta_{\text{rd}}}h_{\text{rd}})\right) \quad (45)$$

$$f_2'(\alpha) = pQ\left(k'(\sqrt{\alpha}h_{\text{sd}} - \sqrt{(1-\alpha)\beta_{\text{rd}}}h_{\text{rd}})\right) = Q\left(k_1\sqrt{\alpha}\right)Q\left(k'(\sqrt{\alpha}h_{\text{sd}} - \sqrt{(1-\alpha)\beta_{\text{rd}}}h_{\text{rd}})\right) \quad (46)$$

where the constant k_1 is given in (36). We observe that the functions $f_1'(\alpha)$ and $f_2'(\alpha)$ are the same as the functions $f_1(\alpha)$ and $f_2(\alpha)$ given in (34) and (35) except for the fact that k is now replaced by k'. Therefore, the solution to the power allocation strategy for M-PPM with $M > 2$ can be obtained from (38) where k, $f_1(\alpha)$ and $f_2(\alpha)$ need to be replaced by k', $f_1'(\alpha)$ and $f_2'(\alpha)$, respectively. For high SNRs, (39) can be applied where k must be replaced by k'.

Note that the proposed cooperative system can be coupled with two possible power allocation schemes. In the first one, α is held constant independently from the specific channel realization while the second scheme is based on adapting the value of α to the channel realization according to the strategy proposed previously in this section. The advantage of the first scheme resides in its simplicity while the second scheme has the capability of achieving higher performance levels as shown later. A possible implementation of the second scheme can be based on evaluating α at D (based on (38)) and providing this value to S and R via two feedback links. In this case, the noise variance as well as the S-R, S-D and R-D channels need to be known at D. For scheme 1, α is held constant and no feedback is required. In this case, R needs to estimate only the S-R channel while the detection at D requires only the knowledge of the R-D and S-D channels. These power allocation strategies (PAS) will be referred to as PAS-1 and PAS-2 in what follows.

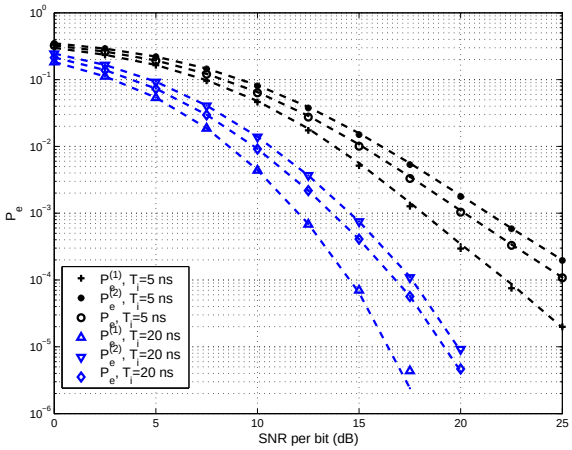

Fig. 3. The different error probabilities with 2-PPM and $(\beta_{\text{sr}}, \beta_{\text{rd}}) = (4, 1)$. PAS-1 is applied with $\alpha = 0.5$. The marked points are obtained by simulations while the dashed curves correspond to the analytical results in (24) and (25).

V. Numerical Results

Simulations are performed over the IEEE 802.15.3a channel model recommendation CM2 [15]. A Gaussian pulse with a duration of $T_w = 0.5$ ns is used. The modulation delay is chosen to verify $\delta = 100$ ns which is larger than the maximum delay spread of the UWB channel. The presented results show the variation of the error probability as a function of the SNR per bit which is equal to $\frac{E_s}{N_0 \log_2 M}$ for non-cooperative systems and to $\frac{E_s}{N_0 \log_2 M}\frac{M+1}{M}$ for the proposed cooperation scheme.

Fig. 3 shows the variations of $P_e^{(1)}$, $P_e^{(2)}$ and P_e given in (31) for 2-PPM with $(\beta_{\text{sr}}, \beta_{\text{rd}}) = (4, 1)$. PAS-1 is applied with $\alpha = 0.5$. This figure shows the close match between simulations and the theoretical analysis presented in Section III despite the fact that the interference term h_{in} was neglected in the theoretical study. This shows that this term can be safely neglected without resulting in significant modifications of the results. Fig. 3 also shows that the performance is limited mainly by $P_e^{(2)}$ which is significantly larger than $P_e^{(1)}$.

Fig. 4 compares the performance of the proposed scheme with that of non-cooperative systems for $M = 2$ and $\beta_{\text{sr}} = \beta_{\text{rd}} = 4$ in the case where PAS-1 is applied with $\alpha = 0.8$. This figure shows the high performance levels and the enhanced diversity orders achieved by the proposed cooperation strategy for different integration times. The obtained numerical results support the theoretical analysis presented in Section III showing

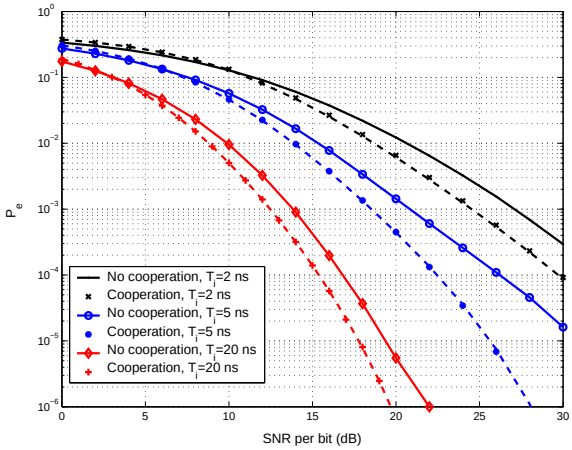

Fig. 4. Performance of the proposed scheme with 2-PPM and $\beta_{\text{sr}} = \beta_{\text{rd}} = 4$. PAS-1 is applied with $\alpha = 0.8$. The marked points are obtained by simulations while the dashed curves correspond to the analytical results in (26) and (31).

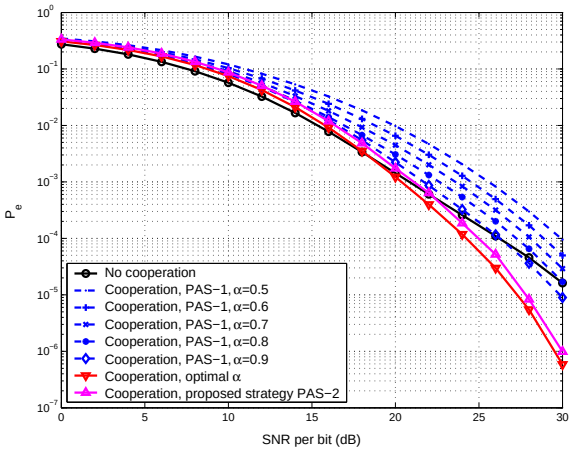

Fig. 6. Impact of power allocation on the performance of the proposed cooperation scheme. PAS-1 and PAS-2 are compared with 2-PPM for $\beta_{\text{sr}} = \beta_{\text{rd}} = 1$ and $T_i = 5$ ns.

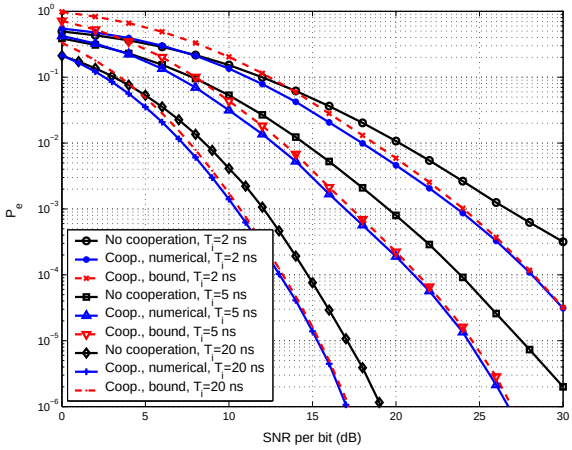

Fig. 5. Performance of the proposed scheme with 4-PPM and $\beta_{\text{sr}} = \beta_{\text{rd}} = 4$. PAS-1 is applied with $\alpha = 0.8$.

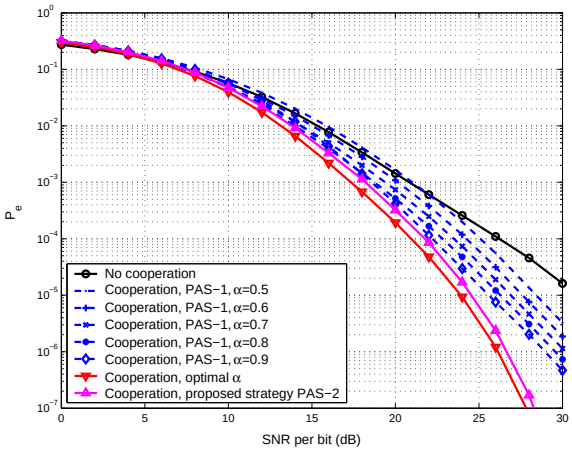

Fig. 7. Impact of power allocation on the performance of the proposed cooperation scheme with 2-PPM for $\beta_{\text{sr}} = \beta_{\text{rd}} = 4$ and $T_i = 5$ ns.

that the performance of the proposed scheme with 2-PPM can be correctly obtained from combining (24), (25), (26) and (31). Note that for $M = 2$, the data rate reduction of the proposed scheme is maximum since the function $\frac{M+1}{M}$ decreases with M. Fig. 4 shows that even in this extreme case, the proposed cooperation strategy outperforms non-cooperative systems for practically all values of the SNR.

Fig. 5 shows the performance with $M = 4$ and $\beta_{\text{sr}} = \beta_{\text{rd}} = 4$. PAS-1 is applied with $\alpha = 0.8$. This figure shows that the upper-bound given in (28) can be accurately used for estimating the performance of the proposed scheme with M-PPM (for $M > 2$) especially for large values of the SNR since this bound is very close to the exact error probability for large SNRs. Note that even for the large integration time of $T_i = 20$ ns where the number of multi-path components captured at the receiver side is large, the proposed scheme results in a performance gain of about 1.7 dB at $P_e = 10^{-3}$.

Fig. 6 compares the power allocation strategies PAS-1 and PAS-2 with 2-PPM and $T_i = 5$ ns. In this figure, we consider the extreme case where the relay is as far from the source and destination as the destination is from the source, i.e. $\beta_{\text{sr}} = \beta_{\text{rd}} = 1$. This figure shows that in this case where there is no power gain in the system, applying the proposed cooperation strategy with PAS-1 might not be useful. In fact, for practical values of the SNR not exceeding 30 dB, the proposed cooperative scheme (associated with PAS-1) degrades the performance for $\alpha = 0.5, \ldots, 0.8$ while small performance gains are observed for SNRs exceeding 26 dB for $\alpha = 0.9$. This figure shows the importance of adapting the transmitted power to the specific channel state based on PAS-2. This allows the proposed cooperative scheme to outperform non-cooperative systems for SNRs exceeding 18.5 dB. This figure also shows the efficiency of the proposed suboptimal, yet simple, power allocation strategy described in (38). In fact, the gap between the optimal and suboptimal strategies does not exceed 0.8 dB for any value of the SNR. The obtained results also highlight the important fact that the proposed power allocation strategy PAS-2 does not penalize the diversity order that can be achieved by the proposed cooperative scheme. In fact, the error curves pertaining to the optimal and suboptimal strategies have the same slope as well as similar variations except for a small bias in the SNR.

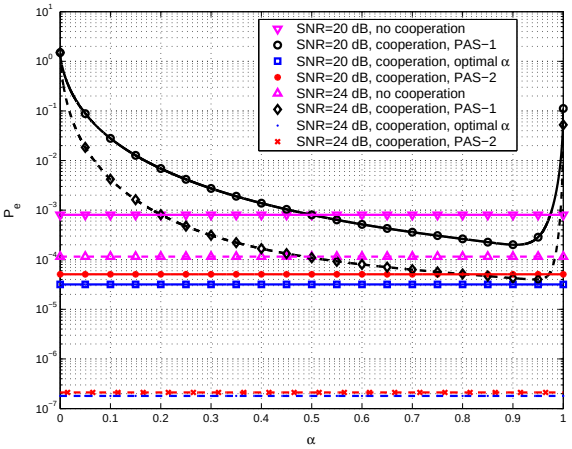

Fig. 8. Impact of power allocation on the performance of the proposed cooperation scheme with 4-PPM for $\beta_{\text{sr}} = \beta_{\text{rd}} = 4$ and $T_i = 5$ ns.

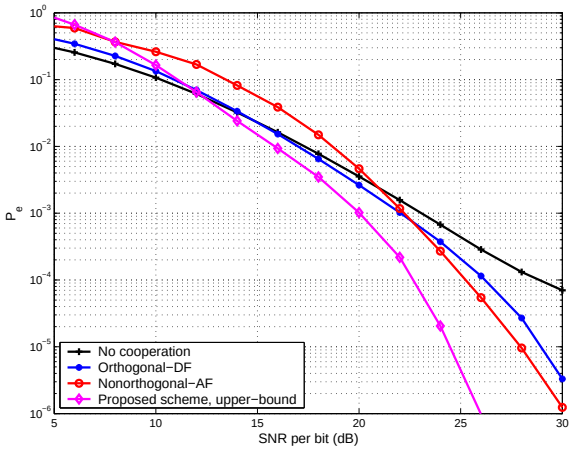

Fig. 9. PAS-2 versus the nonorthogonal-AF and orthogonal-DF schemes in [6] and [10]. 8-PPM is deployed with $\beta_{\text{sr}} = \beta_{\text{rd}} = 4$ and $T_i = 3$ ns.

The same simulation setup is reproduced in Fig. 7 with $\beta_{\text{sr}} = \beta_{\text{rd}} = 4$. In this case, applying PAS-1 results in significant performance gains that are highly dependent on the specific value of α. For example, setting $\alpha = 0.5$ results in a performance gain of about 1.1 dB at $P_e = 10^{-4}$ while this performance gain increases to 4 dB for $\alpha = 0.9$. As in Fig. 6, the superiority of the proposed power allocation strategy (that is very close to the optimal strategy) is confirmed in Fig. 7.

Fig. 8 compares the power allocation strategies PAS-1 and PAS-2 with 4-PPM, $T_i = 5$ ns and $\beta_{\text{sr}} = \beta_{\text{rd}} = 4$. This figure shows that the performance levels that can be achieved by PAS-1 are highly dependent on the specific value of α. At SNR=24 dB, the best performance that can be obtained from associating the proposed cooperation scheme with PAS-1 is $P_e = 4 \times 10^{-5}$ for $\alpha = 0.95$. On the other hand, PAS-2 is capable of drastically reducing this value to about 2×10^{-7}. Finally, the obtained results show that the proposed power allocation strategy PAS-2 can achieve error probabilities that are very close to those achieved by the optimal strategy.

Fig. 9 compares the proposed cooperation strategy with the nonorthogonal-AF and orthogonal-DF schemes in [6] and [10]. 8-PPM is deployed with $\beta_{\text{sr}} = \beta_{\text{rd}} = 4$ and $T_i = 3$ ns. The performance of the proposed cooperation scheme, that is associated with PAS-2, is determined from the upper-bound in (28). Results show the superiority of the proposed scheme especially for large SNRs. In fact, this scheme avoids the joint decoding and noise amplification of [6] as well as the $1/2$ data-rate reduction of [10].

VI. Conclusion

Compared to the classical QAM and PAM modulations deployed in narrow-band and UWB systems, the structure of the PPM constellations constitutes an additional degree of freedom that can be exploited in the construction of novel cooperation protocols. In this work, we have taken the structure of these constellations into consideration and constructed a simple and powerful symbol-by-symbol cooperative diversity scheme that drastically simplifies the structure of the relay and the destination compared to the conventional AF and DF protocols. Our work also highlighted the importance of power allocation in such UWB cooperative systems; this constituted an important design parameter that turned out to be critical in determining the system performance. Finally, we hope that this work will motivate more research effort in this direction.

Appendix

The conditional SEP can be written as: $P_{e|H} = \frac{1}{M}\sum_{m=1}^{M} P_{e|H}^{(m)}$ where $P_{e|H}^{(m)}$ stands for the conditional SEP given that the PPM symbol $m \in \{1, \ldots, M\}$ was transmitted. This probability can be written as: $P_{e|H}^{(m)} = \sum_{i=1}^{M+1} p_i^{(m)} P_i^{(m)}$ where $P_i^{(m)}$ stands for error probability given that the symbol m was transmitted while the relay is forwarding the symbol $i \in \{1, \ldots, M\}$ (in slot $i+1$); the case $i = M+1$ corresponds to the case where the relay is backing off. Finally, $p_i^{(m)}$ stands for the probability of the relay forwarding the symbol $\hat{m} = i$ while the source is transmitting the symbol m.

For $i \neq M+1$, the probability $p_i^{(m)}$ is given by: $p_i^{(m)} = \prod_{k=1}^{i-1} \Pr(y_{\text{r}}^{(k)} < I_{th}) \Pr(y_{\text{r}}^{(i)} \geq I_{th})$. Given that $y_{\text{r}}^{(m)} = h_1 + n_{\text{r}}^{(m)}$ while $y_{\text{r}}^{(m')} = n_{\text{r}}^{(m')}$ for $m' \neq m$, then for $i < m$:

$$p_i^{(m)} = \prod_{k=1}^{i-1} \Pr(n_{\text{r}}^{(k)} < I_{th}) \Pr(n_{\text{r}}^{(i)} \geq I_{th}) = (1-p)^{i-1} p \quad (47)$$

following from (15).

For $i = m$, following from (14) and (15):

$$\begin{aligned} p_i^{(m)} &= \prod_{k=1}^{i-1} \Pr(n_{\text{r}}^{(k)} < I_{th}) \Pr(h_1 + n_{\text{r}}^{(m)} \geq I_{th}) \\ &= (1-p)^{i-1}(1-p) = (1-p)^i \end{aligned} \quad (48)$$

In the same way, for $m < i \leq M$:

$$\begin{aligned} p_i^{(m)} &= \prod_{k=1}^{m-1} \Pr(n_{\text{r}}^{(k)} < I_{th}) \Pr(h_1 + n_{\text{r}}^{(m)} < I_{th}) \\ &\quad \times \prod_{k=m+1}^{i-1} \Pr(n_{\text{r}}^{(k)} < I_{th}) \Pr(n_{\text{r}}^{(i)} \geq I_{th}) \\ &= (1-p)^{m-1} p (1-p)^{i-m-1} p = (1-p)^{i-2} p^2 \end{aligned} \quad (49)$$

For $i = M+1$, $p_i^{(m)} = \prod_{k=1}^{M} \Pr(y_{\rm r}^{(k)} < I_{th})$ resulting in:

$$p_i^{(m)} = \prod_{k=1}^{m-1} \Pr(n_{\rm r}^{(k)} < I_{th}) \Pr(h_1 + n_{\rm r}^{(m)} < I_{th}) \prod_{k=m+1}^{M} \Pr(n_{\rm r}^{(k)} < I_{th}) = (1-p)^{m-1} p (1-p)^{M-m} = (1-p)^{M-1} p = (1-p)^{i-2} p \quad (50)$$

Now combining (47)-(50) results in (30).

Given that symbol m is transmitted by the source and symbol i is transmitted by the relay, then (neglecting the interference) the decision variables at the destination can be written as:

$$y_{\rm d}^{(j)} = \delta_{j,m} h_2 + \delta_{j,i} h_3 + n_{\rm d}^{(j)} \quad ; \quad j = 1, \ldots, M \quad (51)$$

In this case, the error probability $P_i^{(m)}$ can be written as:

$$P_i^{(m)} = \Pr\left(\bigcup_{j=1 \ ; \ j \neq m}^{M} (y_{\rm d}^{(j)} \geq y_{\rm d}^{(m)}) \right) \leq \sum_{j=1 \ ; \ j \neq m}^{M} \Pr(y_{\rm d}^{(j)} > y_{\rm d}^{(m)}) \triangleq \sum_{j=1 \ ; \ j \neq m}^{M} P_{i,j}^{(m)} \quad (52)$$

where the union bound was invoked. From (51), for $j \neq m$:

$$P_{i,j}^{(m)} = \Pr\left(\delta_{j,i} h_3 + n_{\rm d}^{(j)} > h_2 + \delta_{m,i} h_3 + n_{\rm d}^{(m)} \right) = \Pr\left(n_{\rm d}^{(j)} - n_{\rm d}^{(m)} > h_2 + (\delta_{m,i} - \delta_{j,i}) h_3 \right) \quad (53)$$

For $j \neq m-1$ and $j \neq m+1$, the noise terms $n_{\rm d}^{(j)}$ and $n_{\rm d}^{(m)}$ are uncorrelated following from (10). In this case, (53) can be written as:

$$P_{i,j}^{(m)} = Q\left(\frac{h_2 + (\delta_{m,i} - \delta_{j,i}) h_3}{\sqrt{2 \frac{N_0}{2} (h_{\rm sd} + h_{\rm rd})}} \right) \quad ; \quad j \neq m \pm 1 \quad (54)$$

For $j = m-1$ or $j = m+1$, $\mathrm{E}[n_{\rm d}^{(j)} n_{\rm d}^{(m)}] = \frac{N_0}{2} \sqrt{h_{\rm sd} h_{\rm rd}}$ following from (10). Following an analysis similar to the one given in (17)-(21) shows that (53) can be written in this case as:

$$P_{i,j}^{(m)} = Q\left(\frac{h_2 + (\delta_{m,i} - \delta_{j,i}) h_3}{\sqrt{2 \frac{N_0}{2} (h_{\rm sd} + h_{\rm rd} - \sqrt{h_{\rm sd} h_{\rm rd}})}} \right) \quad ; \quad j = m \pm 1 \quad (55)$$

Finally, combining (54) and (55) and replacing h_2 and h_3 by their values results in (29).

REFERENCES

[1] L. C. Wang, W. C. Liu, and K. J. Shieh, "On the performance of using multiple transmit and receive antennas in pulse-based ultrawideband systems," *IEEE Trans. Wireless Commun.*, vol. 4, pp. 2738–2750, November 2005.

[2] C. Abou-Rjeily, "Pulse antenna permutation and pulse antenna modulation: two novel diversity schemes for achieving very high data-rates with unipolar MIMO-UWB communications," *IEEE J. Select. Areas Commun.*, vol. 27, no. 8, pp. 1331 – 1340, 2009.

[3] A. Sendonaris, E. Erkip, and B. Aazhang, "User cooperation diversity. Part I. System description," *IEEE Trans. Commun.*, vol. 51, no. 11, pp. 1927 – 1938, November, 2003.

[4] ——, "User cooperation diversity. Part II. Implementation aspects and performance analysis," *IEEE Trans. Commun.*, vol. 51, no. 11, pp. 1939 – 1948, November, 2003.

[5] J. Laneman and G. Wornell, "Distributed space time coded protocols for exploiting cooperative divesrity in wireless networks," *IEEE Trans. Inform. Theory*, vol. 49, no. 10, pp. 2415–2425, October 2003.

[6] C. Abou-Rjeily, N. Daniele, and J. C. Belfiore, "On the amplify-and-forward cooperative diversity with time-hopping ultra-wideband communications," *IEEE Trans. Commun.*, vol. 56, no. 4, pp. 630 – 641, April 2008.

[7] C. Abou-Rjeily and W. Fawaz, "Distributed information-lossless space-time codes for amplify-and-forward TH-UWB systems," *IEEE Commun. Lett.*, vol. 12, no. 4, pp. 298 – 300, April 2008.

[8] K. Maichalernnukul, F. Zheng, and T. Kaiser, "Design and performance of dual-hop MIMO UWB transmissions," *IEEE Trans. Veh. Technol.*, vol. 59, no. 6, pp. 2906 – 2920, July 2010.

[9] C. Yalcin and M. Koca, "Space-time coded user cooperation for ultra-wideband systems," in *Proceedings IEEE International Conference on Ultra-Wideband (ICUWB2008)*, vol. 3, 2008, pp. 135–138.

[10] C. Abou-Rjeily, N. Daniele, and J. C. Belfiore, "On the decode-and-forward cooperative diversity with coherent and non-coherent UWB systems," in *Proceedings IEEE Conference on UWB*, September 2006, pp. 435 – 440.

[11] K. Maichalernnukul, T. Kaiser, and F. Zheng, "On the performance of coherent and noncoherent UWB detection systems using a relay with multiple antennas," *IEEE Trans. Wireless Commun.*, vol. 8, no. 7, pp. 3407 – 3414, July 2009.

[12] Z. Zeinalpour-Yazdi, M. Nasiri-Kenari, and B. Aazhang, "Bit error probability analysis of UWB communications with a relay node," *IEEE Trans. Wireless Commun.*, vol. 9, no. 2, pp. 802 – 813, February 2010.

[13] W. Siriwongpairat, W. Su, Z. Han, and K. Liu, "Employing cooperative diversity for performance enhancement in UWB communication systems," in *Proceedings IEEE Wireless Communications and Networking Conference*, vol. 4, 2006, pp. 1854 – 1859.

[14] Z. Zeinalpour-Yazdi, M. Nasiri-Kenari, B. Aazhang, J. Wehinger, and C. Mecklenbrauker, "Bounds on the delay-constrained capacity of UWB communication with a relay node," *IEEE Trans. Wireless Commun.*, vol. 8, no. 5, pp. 2265 – 2273, May 2009.

[15] J. Foerster, "Channel modeling sub-committee Report Final," Technical report IEEE 802.15-02/490, IEEE 802.15.3a WPANs, 2002.

Chadi Abou-Rjeily received his B.S. degree in computer and electrical engineering in 2002 from the Lebanese University, Roumieh, Lebanon. He received his M.S. and Ph.D. degrees in electrical engineering in 2003 and 2006 respectively from the " École Nationale Supérieure des Télécommunications (ENST)", Paris, France. From September 2003 to February 2007, he was also a research fellow at the Laboratory of Electronics and Information Technology of the French Atomic Energy Commission (CEA-LETI). Currently, he is an assistant professor at the faculty of engineering and architecture of the Lebanese American University, Byblos, Lebanon. His research interests are in space-time coding, free-space optics and ultra-wideband communications.